Effect of Poly(methyl methacrylate) Addition on the Dielectric and Energy Storage Properties of Poly(vinylidene fluoride)

Qingjie Meng,[1] Wenjing Li,[1] Yuansuo Zheng,[1,2] Zhicheng Zhang[1,2]

[1]*Department of Applied Chemistry, School of Science, Xi'an Jiaotong University, Xi'an 710049, People's Republic of China*
[2]*Ministry of Education (MOE), Key Laboratory for Nonequilibrium Synthesis and Modulation of Condensed Matter, Xi'an 710049, People's Republic of China*

Received 20 September 2009; accepted 10 November 2009
DOI 10.1002/app.31777
Published online 27 January 2010 in Wiley InterScience (www.interscience.wiley.com).

ABSTRACT: Poly(methyl methacrylate) (PMMA) was introduced into poly(vinylidene fluoride) (PVDF) via a solution blending process, and a series of PVDF/PMMA blends were obtained in an effort to reduce the energy loss of pure PVDF. The effects of the composition and thermal treatment on the properties of the polymer blends were carefully studied. The results show that the introduction of PMMA led to a lower crystallinity and a smaller crystal size of PVDF for its dilution effect. As a result, the dielectric constant and energy storage density of the polymer blends were slightly reduced. Meanwhile, the phase transition of the PVDF crystals from the α phase to the β phase happened during the quenching of the blend melt to ice–water; this was also observed in the untreated or annealed blends with PMMA contents over 50 wt %. Compared with the α-PVDF, the PVDF crystals in the β phase possessed a lower melting temperature, a higher dielectric constant, and a lower dielectric loss. The addition of PMMA reduced the energy loss of PVDF significantly, whereas the energy storage density decreased slightly. The optimized blend film with about 40 wt % PMMA and PVDF in the β phase showed a relative high energy storage density and the lowest energy loss. © 2010 Wiley Periodicals, Inc. J Appl Polym Sci 116: 2674–2684, 2010

Key words: blends; crystal structures; ferroelectricity; fluoropolymers

INTRODUCTION

Poly(vinylidene fluoride) (PVDF) and poly(vinylidene fluoride-co-trifluoroethylene) [P(VDF-TrFE)] are well-known ferroelectric polymers with excellent pyroelectric and piezoelectric properties and have been extensively used as electrochemical sensors, actuators, and transducers.[1] Recently, because of the increasing demand for dielectric polymers with high dielectric constants for high-pulse energy storage applications, a lot of research interest has turned to the modification of PVDF-based fluoropolymers.[2] Because the ferroelectric–paraelectric transition temperature (Curie temperature) of the β-PVDF and P(VDF–TrFE) is much higher than ambient temperature, depending on the composition, these polymers exhibit ferroelectric properties at room temperature, which means their displacement–electric field (D–E) hysteresis loops are near rectangle shape. Therefore, they possess a high remnant polarization (~0.1 C/m^2) and render a rather small energy density. For energy storage capacitor applications, they have to be turned into paraelectric polymers featured with slim D–E hysteresis loops, which favor the release of stored energy and reduce the energy loss.

Since the end of the last century, different methods have been reported for the modification of PVDF or P(VDF–TrFE), and a series of PVDF-based copolymers and terpolymers with reduced ferroelectric–paraelectric transition temperatures have been successfully prepared. For example, electron irradiation was first reported to modify P(VDF–TrFE) in 1998.[2(d)] Via the breakage of the large crystal into small ones with high-energy electron beams, the Curie temperature of irradiated P(VDF–TrFE) was shifted to room temperature, and D–E hysteresis loops at room temperature were turned from a rectangle shape into a slim circle. Another well-known method is the incorporation of another monomer (i.e., chlorotrifluoroethylene or chlorodifluoroethylene) to form a kink in the resulting polymer chain and hinder the formation of large crystals, which was first reported in 2001.[3] This method has been widely applied to obtain paraelectric fluoropolymers and is expected to be the best way to prepare dielectric fluoropolymers for energy storage applications. More recently, an energy storage study showed that

Correspondence to: Z. Zhang (zhichengzhang@mail.xjtu.edu.cn).
Contract grant sponsor: Natural Science Fund Committee of China; contract grant number: 50903065.

the resulting copolymer (poly(vinylidene fluoride-co-chlorotrifluoroethylene) [P(VDF-CTFE)]) and terpolymer [P(VDF–TrFE–CTFE) or P(VDF–TrFE–CDFE)] had a energy density of over 13 J/cm^3 under a 500–600 MV/m electric field,[4] which was several times higher than that of the currently applied dielectric polymer (i.e., that of biaxially oriented polypropylene is about 2.5 J/cm^3 under a 600 MV/m electric field). These exciting results have attracted a lot of research interest, both in academics and industry. However, the high energy loss (ca. 30% of overall energy stored) and the high cost of these polymers limit their application in much wider fields.

The fundamental idea of turning a ferroelectric polymer into paraelectric polymer is to reduce the crystal size of the PVDF-based fluoropolymer and provide sufficient free space for the flipping of the polar crystal. During the flipping of these dipoles following the electric field, the internal friction induced is where the major energy loss comes from. In these semicrystalline polymers, two parts, including a crystal phase and an amorphous phase, exist. We reported that the polarization of the crystal section provided the major contribution for reversible polarization in our previous work, whereas the polarization relaxation of the amorphous phase requires a much longer period and results in a large energy loss.[4(e)] Therefore, it is crucial to enhance the energy density and minimize the energy loss to reduce the relaxation time of the amorphous section and to maintain the high polarization of the crystal part. In this study, poly(methyl methacrylate) (PMMA) was blended with PVDF to achieve these two goals. First, the dilution effect of PMMA reduced the crystal size and crystallinity of PVDF in the resulting polymer, which was the key to the realization of high energy storage and was achieved via the incorporation of another comonomer. Second, the introduction of PMMA with a high glass-transition temperature, instead of amorphous PVDF in the elastic state, was expected to reduce the relaxation time of the amorphous phase and, therefore, reduce the energy loss of the final product. So far, few studies have been reported on the dielectric constant and energy storage properties of PVDF/PMMA blends, although this blending system is well known and its thermal and crystallization properties have been well investigated.[5] PMMA/PVDF polymer blend thin films were prepared via a solution mixing and casting process. The effects of the composition, thermal treatment, and crystallinity properties on the dielectric and energy storage properties were studied carefully.

EXPERIMENTAL

Materials

PVDF (Solef 6010) in powder was purchased from Shanghai Alliedneon New Materials Co., Ltd. (Shanghai, China) PMMA powder with a molecular weight of 410,000 was purchased from Alfa Aesar China (Tianjin) Co., Ltd. All of the other chemicals were commercially available and were used as received.

Process of film preparation

Films with a thickness of about 20 μm were deposited by the solution-casting method as follows.

A polymeric blend solution containing about 4 wt % polymer was prepared via the dissolution of the polymers in *N*,*N*-dimethylformamide (DMF) at 50°C for 12 h under vigorous stirring. Polymer films were obtained via the casting of the polymeric solution on glass slides at 120°C until the solvent was evaporated completely. The films were cooled to room temperature slowly and peeled off of the substrate, which were marked as untreated samples. Before they were peeled off of the glass substrates, the untreated samples were kept in an oven at 190°C for 10 min followed by quenching in ice–water or cooled to room temperature over 24 h. The films obtained were marked as quenched and annealed samples, respectively. Samples with different compositions were named with the initial capital letter of their thermal treatment followed by their PMMA weight percentage as a subscript; for example, $U_{0.25}$ refers to the untreated film with 25 wt % PMMA, $A_{0.3}$ refers to the annealed film containing 30 wt % PMMA, and $Q_{0.0}$ is the quenched neat PVDF film.

Characterization

IR spectra were obtained on a Fourier transform Nicolet AVATAR 360 Fourier transform infrared (FTIR) instrument (Thermo Nicolet Corp., USA) in the 400–4000 cm^{-1} wave-number range. X-ray diffraction (XRD) analysis was conducted on a Rigaku D/MAX-2400 (Rigaku Industrial Corp., Tokyo, Japan). The wavelength of the X-ray was 1.542 Å (Cu Kα radiation, 40 kV and 100 mA), and the scanning velocity was 10°/min. Differential scanning calorimetry (DSC) analysis was conducted on a Netzsch DSC 200 PC (Netzsch Corp., Selb, Germany) under a nitrogen atmosphere to measure the melting temperature and crystallinity, and the temperature was programmed to rise from 20 to 200°C at a heating speed of 10°C/min. The crystalline modality and crystal size were obtained with a polarizing optical microscope (XP600, Wang Heng Precision Instrument Corp., Shanghai, China).

For electric characterizations, gold electrodes (thickness ≈ 80 nm) were sputtered on both surfaces of the polymer films with a JEOL JFC-1600 Auto fine coater (Japan). The dielectric properties were measured at different frequencies and at 1 V on an HP (4284A) loop inductance, capacitance, resistance

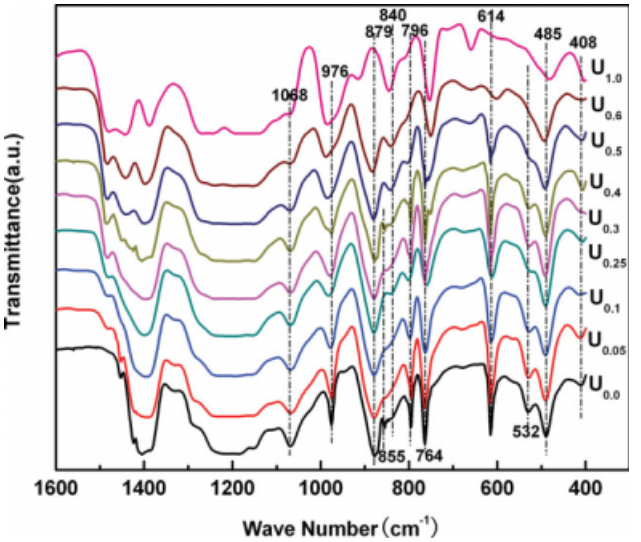

Figure 1 FTIR spectra of the untreated PMMA/PVDF thin films with various PMMA contents. All of the unindicated peaks were common to all three phases. [Color figure can be viewed in the online issue, which is available at www.interscience.wiley.com.]

(LCR) meter. The electric D–E hysteresis loops were measured with a modified Sawyer–Tower circuit and a linear variable differential transducer driven by a lock-in amplifier (Stanford Research Systems, model SR830, USA). Electric fields ranging from 50 to 600 MV/m were applied across the polymer film with an amplified ramp waveform at 10 Hz.

RESULTS AND DISCUSSION

FTIR

The crystalline phases of PVDF were characterized by the infrared absorption bands between 400 and 1000 cm^{-1}.[6] The bands at 485 and 879 cm^{-1} were attributed to the amorphous phase of PVDF and could not be used to identify any of the crystalline phases. The bands at 410, 532, 614, 764, 796, 855, and 976 cm^{-1} were associated with the α phase of PVDF. The bands at 444 and 510 cm^{-1} were characteristic of the β phase, and those at 431, 512, 776, 812, and 833 cm^{-1} were related to the γ phase. The 840 cm^{-1} band was common to the β and γ phases. A sharp and well-resolved band indicated the β phase, whereas a broad band indicated the γ phase. This broad band was due to overlapping with the 833 cm^{-1} band, which frequently appears as a shoulder.[6(g),7]

FTIR spectroscopy was used to study the crystal structure of the untreated polymer blends, as shown in Figure 1. When the PMMA content was lower than 50 wt %, the peaks associated with the α phase of PVDF at 410, 532, 614, 764, 796, 855, and 976 cm^{-1} were very sharp, which indicated that the crystalline phase of PVDF in the polymer blends was mainly in the α phase. Although PMMA addition was over 50 wt %, these peaks disappeared, and new peaks appeared at 430–440 and 840 cm^{-1}, which suggested the formation of the β phase. It has been reported that a PVDF film cast from a DMF solution at a higher temperature (>100°C) favored the formation of the α phase; however, the β phase was generated at a lower temperature, that is, 50°C.[8] Because the film casting temperature was higher than the glass-transition temperature of PMMA, during the solvent evaporation and crystal formation of PVDF, PMMA was always in a viscous state, which showed its limited influence on the crystallization of PVDF. When the PMMA content was sufficiently high, the formation of the α-phase crystals started to be hindered, and only the β phase was observed.

Thermal treatment affected the crystal structure of PVDF as well as the casting temperature and solvent applied. Two kinds of thermal processes, including annealing and quenching in ice–water, were used to treat the films cast from the DMF solution. When the PMMA content was less than 25 wt %, less difference in the FTIR spectra was obtained in the three films processed differently. When the PMMA content was higher than 25 wt %, the bands at 408, 532, 614, 764, 796, 855, and 976 cm^{-1} disappeared, whereas the bands at 440 and 840 cm^{-1} showed up, as shown in Figure 2. Meanwhile, the broad peak at about 490 cm^{-1} was attributed to the overlap of the peaks at 485 cm^{-1} (amorphous PVDF) and 510 cm^{-1} (PVDF in the β phase). These results indicated that the PVDF crystals in the samples quenched in ice–water were mostly in the β phase, although annealing favored the formation of α-PVDF unless PMMA

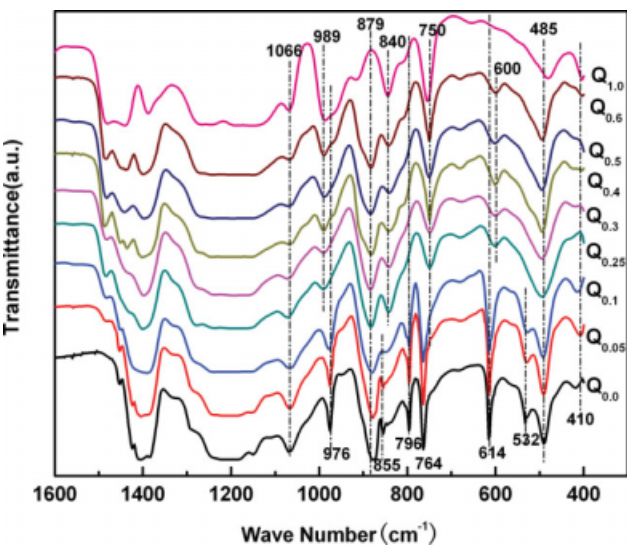

Figure 2 FTIR spectra of the quenched PMMA/PVDF thin films with various compositions. [Color figure can be viewed in the online issue, which is available at www.interscience.wiley.com.]

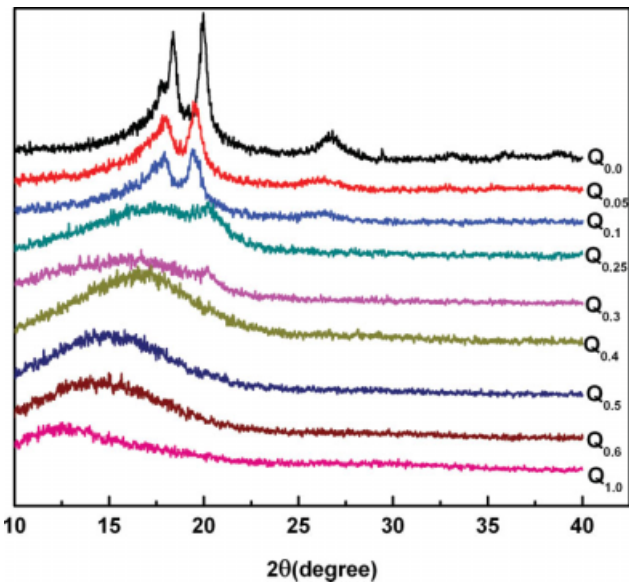

Figure 3 XRD patterns for the quenched PVDF/PMMA blends with different compositions. [Color figure can be viewed in the online issue, which is available at www.interscience.wiley.com.]

content was greater than 50 wt % (the results are not given). It has been well studied that stretching a PVDF film leads to the transition of the α-PVDF to β-PVDF. When the films were melted and quenched immediately, the PVDF crystallization occurred as well as the cooling of the PMMA melt. Because of the shrinking of the PMMA melt during cooling, a stretching strength was formed in the film, and the PVDF polymer chain was *in situ* stretched into a trans-trans-trans-trans (TTTT) conformation; therefore, β-PVDF was formed. However, the stretching strength had to be sufficiently high for the formation of the TTTT conformation of PVDF, which was associated with the content of PMMA. Similar results were also obtained in the PVDF/PMMA blends with 10–20 wt % PMMA, as reported in the literature.[9] During the casting of the films or annealing at high temperature, no stretching occurred as PVDF crystallized; as a result, mostly PVDF in the α phase was formed.

XRD

XRD was another useful method for demonstrating the crystalline phase of PVDF in the blend samples. In Figure 3, the X-ray diffractograms present the quenched blend films with different weight fractions of PMMA. According to the work of Gregorio's group,[6(a)] for pure PVDF, three discernable diffraction peaks appeared at 18.4, 20.0, and 26.8, referent to the diffractions in planes (020), (110), and (021), respectively, all characteristic of the α phase. Another peak appearing at about 40 was the characteristic of the combined (201) and (111) reflections of the β phase, which resulted from molecular defects caused by head–head and tail–tail (HHTT) sequences.[10] When the PMMA content was lower than 10 wt %, the XRD curves of the polymer blends were similar to those of neat PVDF, which indicated that the PVDF crystals were mostly in the α phase. Meanwhile, the broad peak near at about 40 vanished as more PMMA was introduced. As the PMMA content increased to more than 25 wt %, the blends ($Q_{0.25}$–$Q_{0.3}$) had a new peak at about $2\theta = 20.3$, which referred to the diffractions in planes (110) and (200), characteristic of the β phase. Meanwhile, the characteristic peaks of the α phase at 18.4, 20.0, and 26.8 disappeared completely, which meant that the PVDF crystals in these samples were all in the β phase. These results confirm the conclusion obtained from FTIR spectroscopy.

The effect of the thermal treatment on the XRD of PVDF/PMMA containing 25 wt % PMMA is shown in Figure 4. For the untreated sample, the PVDF crystals were completely in the α phase, with characteristic peaks at 18.4, 20.0, and 26.8. After annealing, they were still in the α phase, but the XRD showed a significant difference in the peaks of 18.4 and 20.0. Annealing led to a higher peak at 20.0 and a smaller one at 18.4, corresponding to the diffractions in planes (020) and (110), respectively, which indicated the larger size and thickness of the PVDF crystals in the α phase formed after annealing. After quenching, the characteristic peaks of the α-PVDF crystals completely disappeared, and a new peak at 20.3 appears. This indicated that the PVDF crystals in this blend had completely converted from the α phase to the β

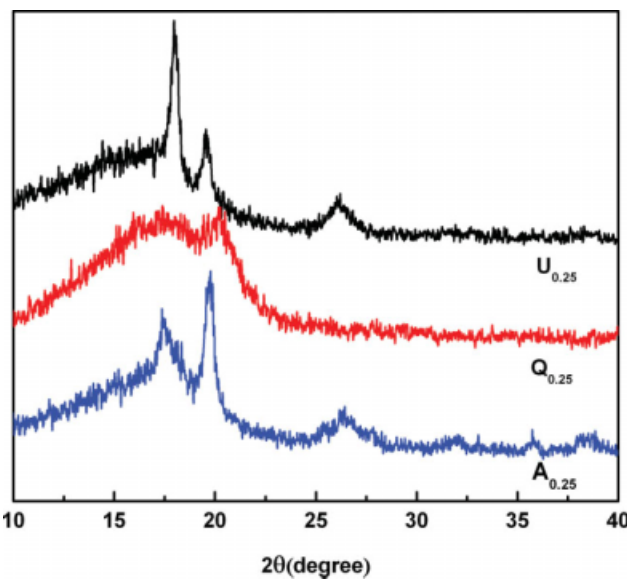

Figure 4 Effect of the thermal treatment on the XRD of the polymer blend containing 25 wt % PMMA. [Color figure can be viewed in the online issue, which is available at www.interscience.wiley.com.]

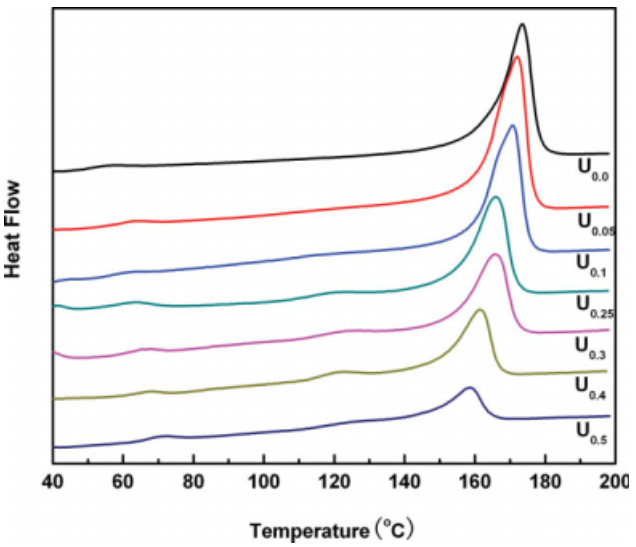

Figure 5 DSC curves of the untreated PVDF/PMMA blends with various compositions. [Color figure can be viewed in the online issue, which is available at www.interscience.wiley.com.]

phase via quenching in ice–water. Meanwhile, the characteristic peak of HHTT PVDF in the β phase appeared around 40° after quenching, which also meant that quenching favored the formation of β-PVDF. This confirmed the results obtained from FTIR spectroscopy, and it was not difficult to deduce that the phase transition also occurred in other samples with higher PMMA contents than 25 wt %.

Thermal analysis

The introduction of PMMA changed the thermal properties of PVDF and its crystallization. The DSC curves of the untreated polymer blends with altered compositions are presented in Figure 5. As the PMMA content increased from 0 to 50 wt %, the melting temperature decreased slightly from 173 to 158°C. The enthalpy of melting decreased from 58.6 to 12.5 J/g. The crystallinity was obtained via the division of the melting enthalpy by 104 J/g. As the PMMA content increased from 0 to 50 wt %, the crystallinity of the polymer decreased from 56.3 to 12.0%; this change was mostly induced by the dilution effect of the introduced PMMA. It was reported that the α and β phases of PVDF crystals possess different melting temperatures and sometimes exhibit multiple peaks on DSC curves.[11] Usually, the melting point of pure α-phase PVDF is at about 170°C,[5(e)] and β-phase PVDF possesses a slightly lower melting temperature, around 161°C.[5(a,c)] Therefore, the decrease in the melting temperature may have been due to the different phases of PVDF in the polymer blends. The results obtained from FTIR and XRD indicate that the PVDF crystals were dominated by the α phase in pure PVDF. As the PMMA content increased, more β-phase PVDF crystals were formed until all of the PVDF crystals were transferred into the β phase in the sample containing over 50 wt % PMMA. As a result, the melting temperature slowly shifted from 170°C to around 160°C.

This phenomenon was further confirmed by the DSC curves observed in the quenched samples, as shown in Figure 6. The melting point of samples containing 0–10 wt % PMMA was around 170°C with a single sharp peak. As shown by the XRD and FTIR results obtained previously, the PVDF crystals in these samples were completely in the α phase. When the PMMA content was higher than 25 wt %, PVDF was completely converted into the β phase. The melting temperature dropped to around 160°C and was characterized by a broad peak, and no future decreased occurred as PMMA increased from 25 to 50 wt %. All of the results strongly support that the melting temperature reduction of the polymer blends containing more PMMA was induced by the continuous PVDF crystal-phase transition from the α phase to the β phase. Meanwhile, the small endotherm around 60°C was well known to be the glass temperature of PVDF/PMMA blends.[12]

Thermal treatment showed a significant influence on the crystallinity of the polymer blends. The annealed samples had quite similar DSC curves and trends as the untreated samples but slightly higher melting temperatures and enthalpies, which indicated a higher crystallinity and larger crystal size. The quenched samples possessed lower enthalpies at lower PMMA contents (<10 wt %) and close enthalpies with untreated samples at higher PMMA

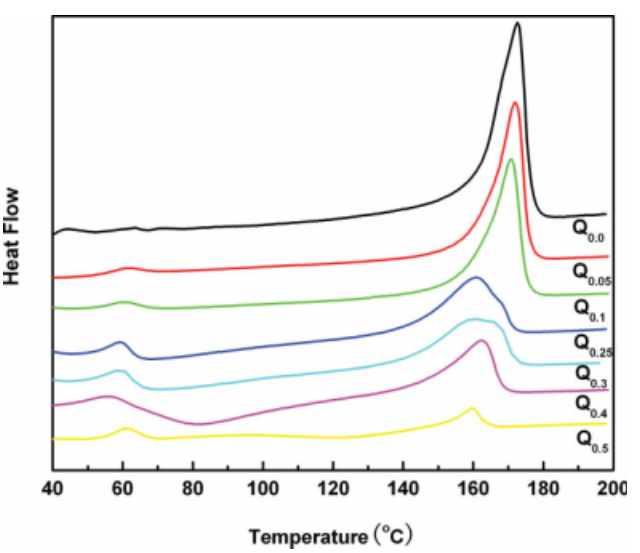

Figure 6 DSC curves of the quenched PVDF/PMMA blends with various compositions. [Color figure can be viewed in the online issue, which is available at www.interscience.wiley.com.]

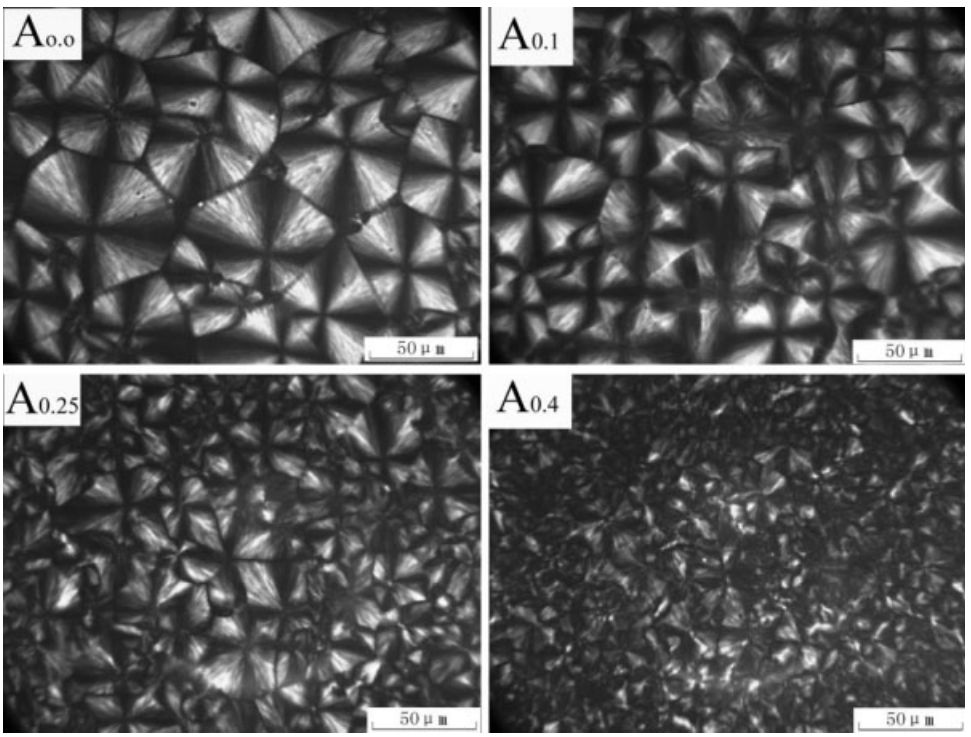

Figure 7 Polarimeter microscope pictures of the PVDF/PMMA blends with various PMMA contents at a magnification of 600×.

contents (>25 wt %). That means quenching did not reduce the crystallinity of the blends significantly once the PMMA content was sufficiently high.

Crystal size of the polymer blends

As discussed previously, annealing was able to cause the formation of larger crystals and improve the crystallinity of the blends. In an effort to obtain more direct evidence, we applied a polarimeter microscope to measure the crystal size. In Figure 7, microscope pictures of pure PVDF [Fig. 7(a)], $A_{0.1}$ [Fig. 7(b)], $A_{0.25}$ [Fig. 7(c)], and $A_{0.4}$ [Fig. 7(d)] at a magnification of 600× are shown. A typical black cross was observed in all of the samples; this was attributed to the α-PVDF spherulites formed. As more PMMA was introduced, the spherulite size decreased. Meanwhile, the crystal part in the polymer blend decreased, and the amorphous part increased. This means that the presence of PMMA hindered the formation of larger spherulite crystals. The distance between the spherulite crystals increased for the dilution effect of PMMA as well. All of the results confirm the conclusion obtained from the DSC results.

The thermal treatment influenced not only the crystallinity and crystal phase of PVDF but also its spherulite structure. In Figure 8, two films ($A_{0.1}$ and $U_{0.1}$) prepared in different processes are presented at the same magnification (600×). Because the spheru-

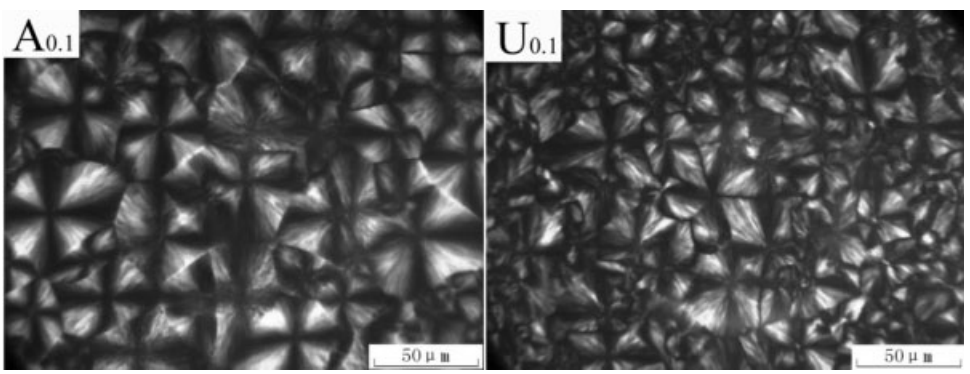

Figure 8 Influence of the thermal treatment on the spherulite structure of the PVDF/PMMA blend containing 10 wt % PMMA (the polarimeter microscope pictures are magnified by 600×).

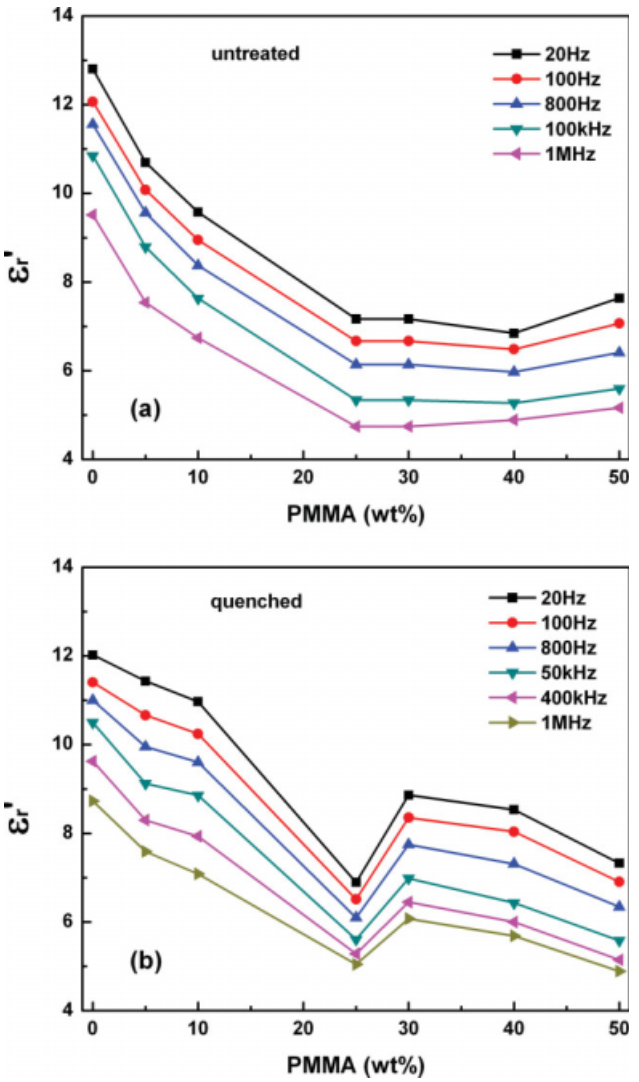

Figure 9 Dielectric constant of PVDF/PMMA with different compositions. [Color figure can be viewed in the online issue, which is available at www.interscience.wiley.com.]

lite was too small to be observed under the polarimeter microscope, even at 600× magnification, the picture of quenched sample is not given. Obviously, smaller PVDF spherulites were observed in the untreated film than in the annealed film. The amorphous part of the untreated film was higher than that of the annealed sample as well.

Dielectric constant and loss

The dielectric constants of the untreated and quenched PVDF/PMMA films with different compositions were measured at 1 V with various frequencies from 20 Hz to 1 MHz, as shown in Figure 9. As the content of PMMA increased, the dielectric constant of the untreated films decreased until the PMMA content was more than 25 wt %. This may have been attributed to the dilution effect of PMMA with a lower dielectric constant (ca. 4) than that of PVDF. A higher dielectric constant was obtained in sample $U_{0.5}$ than in $U_{0.4}$; this may have been because the PVDF crystals were transferred from the nonpolar α phase to the polar β phase, which was already discussed extensively. With the increasing electric field frequency, the dielectric constant of all of the samples is decreased. This was due to the response of different dipole moments of polymer blends to the electric field with varied frequencies, which is discussed in dielectric loss section.

The annealed samples had slightly lower dielectric constants than the untreated polymer blends, which were interpreted by the FTIR and thermal analysis results. Annealing increased the crystal size, as observed in $A_{0.1}$ and discussed previously. However, no obvious crystallinity increase and phase transition were observed. Under the low electric field where the dielectric constant was measured, the response of the PVDF crystals in large size to the electric field was rather weak because the strength provided by the electric field was really small. As a result, samples with a larger crystal size showed lower dielectric constants than those with a smaller crystal size. However, once the samples were quenched, a relative higher dielectric constant was obtained in these samples than in the untreated samples. First, quenching helped to form smaller PVDF crystals, which were more sensitive to the low electric field. Second, the slightly lower crystallinity caused by the quenching did not show much influence on the dielectric constant of the blends for the low polarity of the α-PVDF. Interestingly, when the PMMA content was higher than 25 wt %, the dielectric constant of PVDF/PMMA started to increase and showed a maximum value in the sample $Q_{0.3}$. This may be interpreted by the phase transition from the nonpolar α phase to the polar β phase in these samples, which was discussed previously. Compared to the α-phase crystals, the β PVDF crystals were more sensitive to the low electric field applied. However, proper crystal size is essential for the response of crystals to a low electric field. Therefore, $Q_{0.3}$, with β PVDF crystals and proper crystal size and crystallinity, exhibited a higher dielectric constant.

Dielectric loss is usually used to characterize the motivation of different dipole moments under different electric fields and frequencies. As shown in Figure 10, the tan δ values of untreated [Fig. 10(a)] and quenched [Fig. 10(b)] samples with different compositions were measured at various frequencies. For the pure PVDF, the dielectric loss profile against frequency curve measured at ambient temperature was V-shaped. It was reported that the higher dielectric loss at a lower frequency is due to PVDF crystals and increasing dielectric loss at higher frequencies

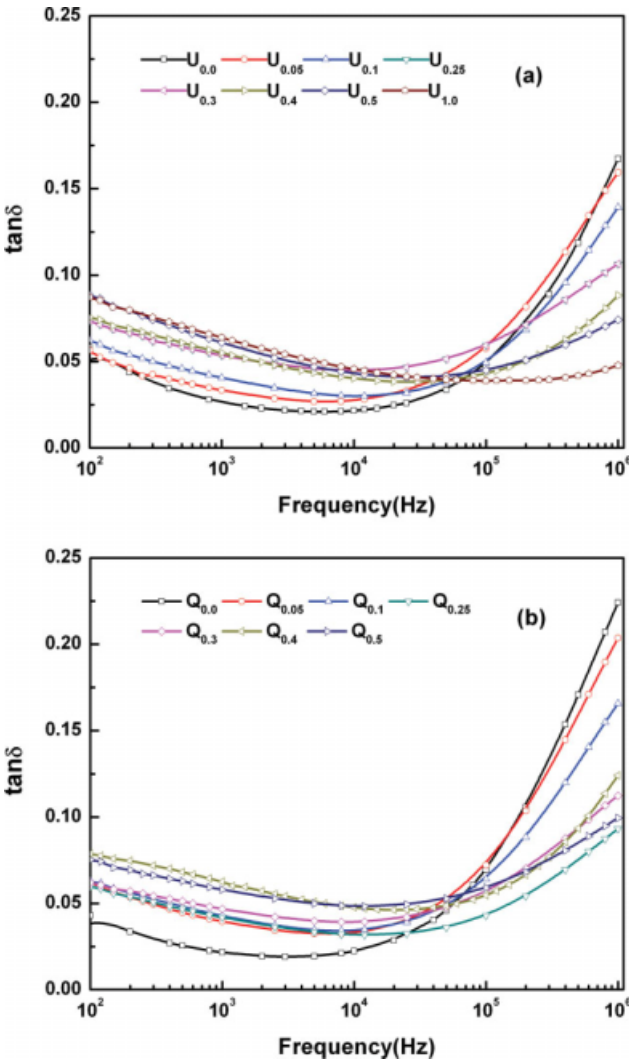

Figure 10 Dielectric loss of the PVDF/PMMA blends against frequency. [Color figure can be viewed in the online issue, which is available at www.interscience.wiley.com.]

corresponds to amorphous PVDF.[5(b)] For the pure PMMA, its dielectric loss decreased continuously as the frequency increased, which we attributed to the extension of the β relaxation of PMMA at lower frequencies.[13] The combination of these three kinds of dipole moment responses to the electric field resulted in the V-shaped dielectric loss profile of PVDF/PMMA against frequency. The dielectric loss of the blends was between that of pure PVDF and PMMA, as shown in Figure 10(a). As the PMMA content increased, the dielectric loss of the blends increased at lower frequencies and decreased at higher frequencies. Annealing did not show much influence on the dielectric loss profiles of PVDF and the polymer blends, whereas quenching led to a significant difference in the dielectric loss profile, as shown in Figure 10(b). As the PMMA content increased, the dielectric loss of samples with 5–30 wt % PMMA at lower frequencies was rather low and close, and $Q_{0.4}$ and $Q_{0.5}$ showed higher dielectric losses. At higher frequencies, tan δ decreased and reached its lowest value when the PMMA concentration was 25 wt %; then, a slightly higher dielectric loss was obtained in samples $Q_{0.3}$–$Q_{0.5}$. That means sample $Q_{0.25}$ possessed the lowest dielectric loss in the full range of frequencies measured; this coincided very well with its low dielectric constant value, as shown in Figure 9(b). Relatively large crystals in the polar β phase have been the cause of this result because the low electric field was not sufficient to pole these large polar crystals, which are very common in ferroelectric P(VDF–TrFE).

D–E loops

Thermal treatment affects the D–E loops of blend films as well as composition does. In Figure 11, the D–E loops of $A_{0.4}$, $U_{0.4}$, and $Q_{0.4}$ are presented. Under the same electric field (100 MV/m), the polarization of the untreated and quenched samples was quite close and was obviously larger than that of the annealed sample. It was reported that the crystal size plays an important role in the polarization of PVDF-based fluoropolymers.[4(d,e)] Under the same electric field, a larger polarization was obtained in fluoropolymers with small crystals because smaller crystals need less space to flip following an electric field. In this case, the quenched and untreated samples possessed a smaller crystal size and lower crystallinity than the annealed sample, as discussed previously; this allowed the PVDF crystals to flip more easily. As a result, a higher polarization was observed, which confirmed the effect of thermal treatment on the dielectric constant discussed

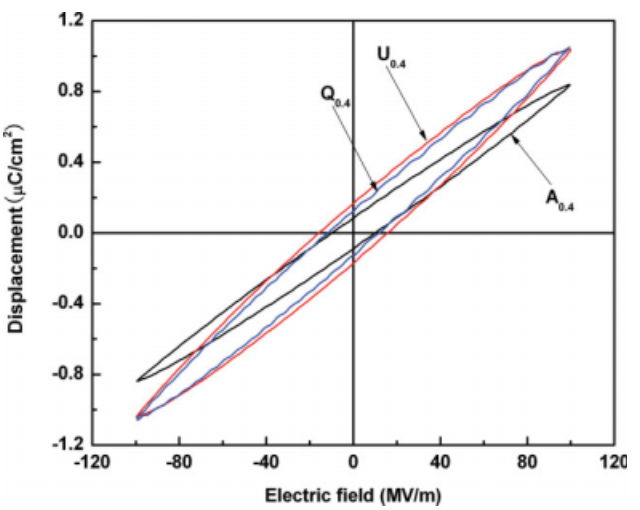

Figure 11 Effect of the thermal treatment on the D–E hysteresis loops of the PVDF/PMMA thin film containing 40 wt % PMMA. [Color figure can be viewed in the online issue, which is available at www.interscience.wiley.com.]

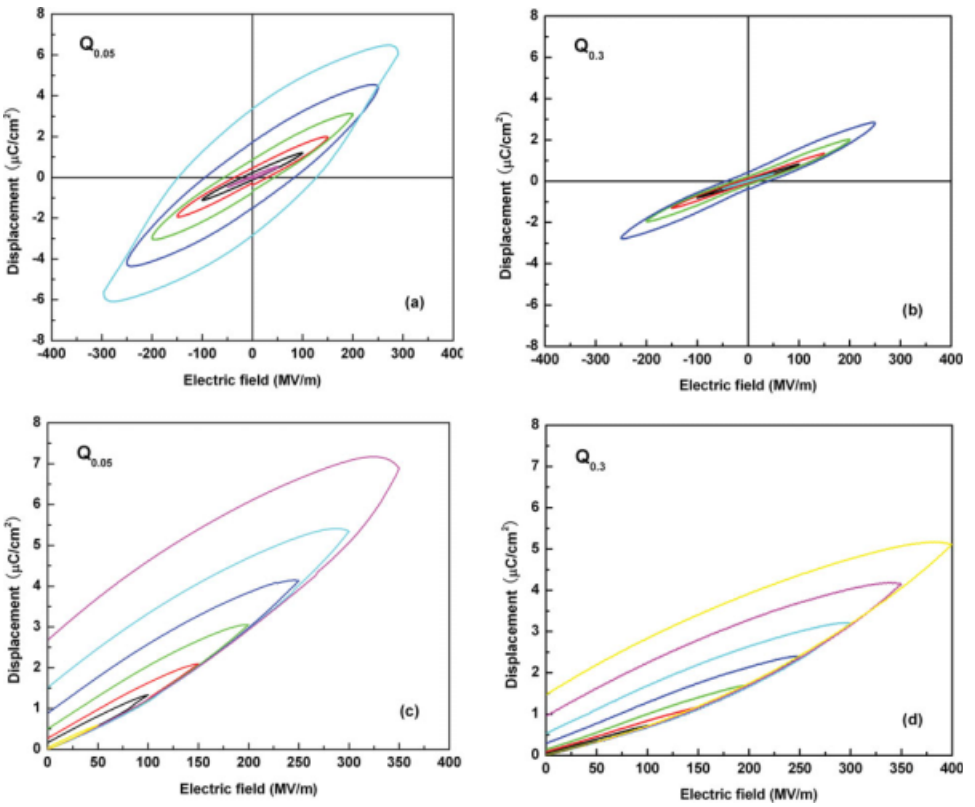

Figure 12 Effect of PMMA on the D–E hysteresis loops of the PVDF/PMMA blends. [Color figure can be viewed in the online issue, which is available at www.interscience.wiley.com.]

previously. Meanwhile, the remnant polarization of the quenched sample was smaller than that of the untreated film, although their polarizations were quite close. This was because the crystallinity was lower, and the polarization of small crystals was easier to reverse once the electric field was removed.

It was reported that the remnant polarization in dipolar D–E loops (Pr_d) of PVDF-based fluoropolymers contains two parts covering the relaxation of small dipoles and the irreversible flip of large crystals.[4(e)] In unipolar D–E loops, only the relaxation of small dipoles can be observed. Therefore, the contribution of large crystals to the remnant polarization can be estimated via the subtraction of the remnant polarization in the unipolar D–E loops (Pr_u) from Pr_d. The value can be used to characterize the contribution of large crystals on the remnant polarization. This is also an important factor for the judgment of paraelectric and ferroelectric materials. A typical PVDF/PMMA unidipolar and dipolar comparison is presented in Figure 12. In sample $Q_{0.05}$, Pr_d (0.035 C/m^2) was much higher than Pr_u (0.016 C/m^2) under a 300 MV/m electric field. This means that the PVDF crystal size was still large and could not flip freely in the polymer blends. As the PMMA content increased to 30 wt % (sample $Q_{0.3}$), Pr_d (0.0045 C/m^2) was much closer to Pr_u (0.0032 C/m^2) under a 250 MV/m electric field. This indicates that the crystals were quite close to the reversible size limit because of the dilution effect of PMMA addition, which was achieved via the incorporation of the comonomer into PVDF or P(VDF–TrFE).

The influence of PMMA on the D–E loops of the PMMA/PVDF quenched blends in an electric field of 300 MV/m is shown in Figure 13. In the same electric field, the displacement of the blends decreased as more PMMA was introduced for its dilution effect. When PMMA content was below 10 wt %, the D–E profiles were more like that of PVDF, which meant that the introduction of PMMA showed less influence on the polymer blends. As the PMMA content increased to over 40 wt %, the D–E profiles were closer to PMMA, which indicated that the PMMA content was so high that the PVDF part was mostly frozen in PMMA. Polymer blends with PMMA contents between 10 and 40 wt % showed special D–E profiles with relatively high polarizations and low remnant polarizations. We previously discussed that the PVDF crystals were mostly in the polar β phase when the PMMA content was higher than 25 wt %. With the assistance of rigid PMMA segments, this kind of crystal was easier to pole and was reversible as the electric field changes. Therefore, a relatively high polarization and a low remnant polarization were obtained in these samples. Meanwhile, the introduction of PMMA with a lower

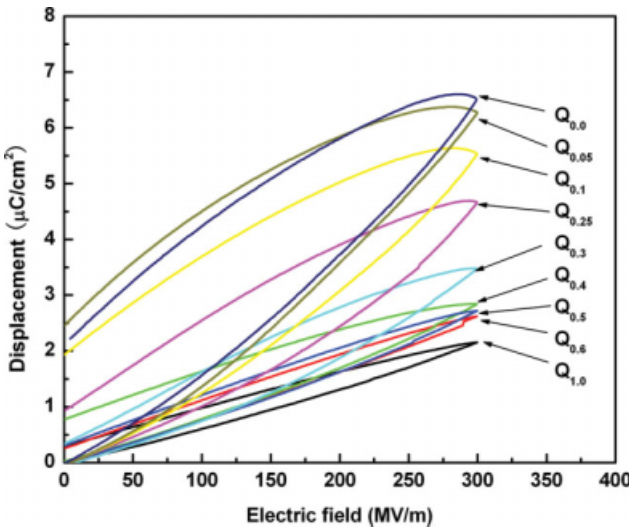

Figure 13 D–E hysteresis loops of the PVDF/PMMA films with different compositions measured under a unipolar electric field. [Color figure can be viewed in the online issue, which is available at www.interscience.wiley.com.]

polarization also led to a lower polarization in PMMA/PVDF, depending on the amount of PMMA added, which confirmed the dielectric constant results discussed previously.

Energy storage and energy loss

For the high-pulse capacitor application purpose, the energy storage and loss properties of the material were mostly of interest. Calculated from unipolar D–E loops via a formula described in the literature;[4(f)] the energy storage density and energy loss of the PVDF/PMMA films are presented in Figure 14. As more PMMA was added to the blends, the energy density decreased continuously. When the PMMA content was over 50 wt %, the energy storage curve coincided with that of pure PMMA, which meant that the contribution of PVDF was negligible and confirmed the results of the D–E loops. This may have been because the PVDF crystal dipole was completely frozen in glass-state PMMA. The energy loss of the PVDF/PMMA films was quite dependent on the electric field because the flipping of the crystals depended not only on the crystal size but also on the electric field. Some crystals could not flip under low electric fields but were able to turn in high electric fields. The flipping and reversing of these crystals caused great internal friction in the films; as a result, a higher energy loss was observed. For the quenched PVDF film cast from DMF, the FTIR results showed that its crystals were in the α phase. When the electric field was below 350 MV/m, more and larger crystals were poled gradually as the electric field increased. Because these α crystals possessed a low polarity, their reversibility was rather poor, and the internal friction was quite high for PVDF with a high crystallinity. As a result, the energy loss was quite high and increased sharply as the electric field increased. When the electric field was greater than 350 MV/m, a phase transition from the α to γ phase occurred, which has been well known and reported.[14] Compared to α-PVDF, PVDF in the γ phase [trans-trans-trans-gauch (TTTG)] possessed a higher polarity and exhibited better reversibility. Therefore, the energy loss was reduced significantly as the electric field improved from 350 to 400 MV/m. A further increase in the electric field led to a higher energy loss once the phase transition was finished. However, when the PMMA content was lower than 25 wt %, most of the PVDF crystals were in the α phase, and the energy loss profile against the electric field was closer to α-PVDF. No phase transition of the PVDF crystals was observed in these samples, as occurs in pure PVDF before breakdown. The presence of a rigid PMMA segment may have hindered the phase transition of the α-PVDF to the γ phase under a high electric field. This may explain the huge energy loss of the samples with PMMA contents less than 25 wt %. When the

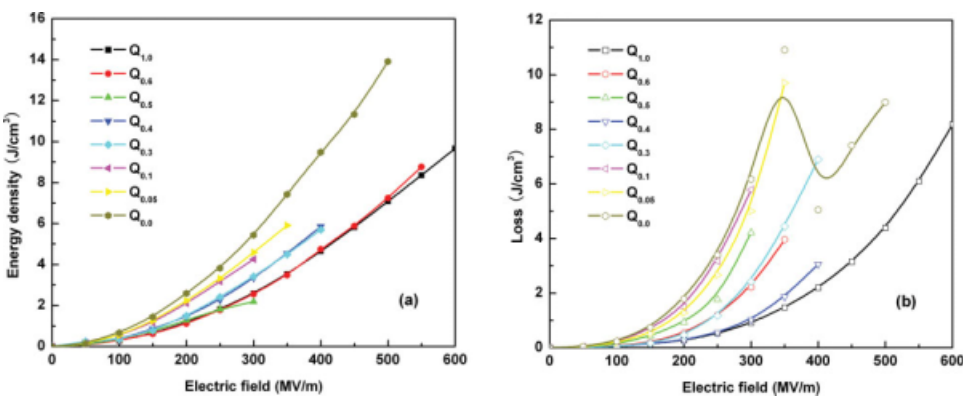

Figure 14 Energy density and loss of quenched PVDF/PMMA blends with different compositions against the electric field. [Color figure can be viewed in the online issue, which is available at www.interscience.wiley.com.]

PMMA content was higher than 25 wt %, the energy loss started to decrease and reached a minimum value in sample $Q_{0.4}$. We have discussed that the PVDF crystals in the quenched samples with PMMA contents over 25 wt % were mostly in the polar β phase, which favored the reversibility of the crystals under electric field. Meanwhile, optimized crystal size was another factor in the realization of the lowest internal friction and, therefore, energy loss. As a result, the sample with 40 wt % PMMA possessed both polar PVDF crystals and a proper crystal size and had a relatively high energy density and the lowest energy loss. That means the optimized composition of the PVDF/PMMA film was about 60/40 wt % when we considered both the energy density and loss.

CONCLUSIONS

Via the solution blending of PMMA with PVDF and different thermal treatment processes, a series of PVDF/PMMA blend films were prepared and characterized. As the PMMA content increased, the crystallinity and crystal size of PVDF decreased. As a result, the enthalpy, dielectric constant, polarization, and energy density of the polymer blends decreased accordingly. This was attributed to the dilution effect of PMMA to PVDF. The phase transition from the nonpolar α phase to the polar β phase induced by PMMA addition and the thermal treatment was another important factor. A high PMMA content and the quenching process favored the PVDF phase transition from α to β. Compared to the α-phase PVDF, the β-PVDF possessed a lower melting temperature, a higher dielectric constant, and a lower dielectric and energy loss. Via the introduction of PMMA into PVDF, the energy loss was significantly reduced, whereas the energy density was slightly reduced. Quenched PVDF/PMMA (60/40 wt %) showed a relatively high energy storage density and the lowest energy loss and was the optimized polymer blend for energy storage purposes.

References

1. (a) Nalwa, H. S. Ferroelectric Polymers; Marcel Dekker: New York, 1995; (b) Lovinger, A. Science 1983, 220, 1115; (c) Wang, T. T.; Herbort, J. M.; Glass, A. M. The Applications of Ferroelectric Polymers; Blackie: Glasgow, 1988; (d) Calleja, F. J. B.; Arche, A. G.; Ezquerra, T. A.; Cruz, C. S.; Batallan, F.; Frick, B.; Cabarcos, E. L. Adv Polym Sci 1993, 108, 1.
2. (a) Macchi, F.; Daudin, B.; Legrand, J. F. Ferroelectrics 1990, 109, 303; (b) Macchi, F.; Daudin, B.; Ermolieff, A.; Marthon, S.; Legrand, J. F. Radiat Effects Defects Solids 1991, 118, 117; (c) daCunha, H. N.; Mattoso, L. H. C.; Faria, R. M. J Polym Sci Part B: Polym Phys 1997, 35, 1201; (d) Zhang, Q. M.; Bharti, V.; Zhao, X. Science 1998, 280, 2101; (e) Karaki, T.; Chou, I. C.; Cross, L. E. Jpn J Appl Phys Regular Pap Short Notes Rev Pap 2000, 39, 5668.
3. (a) Chung, T. C.; Petchsuk, A. Ferroelectr Lett Sect 2001, 28, 135; (b) Chung, T. C.; Petchsuk, A. Macromolecules 2002, 35, 7678; (c) Xu, H. S.; Cheng, Z. Y.; Olson, D.; Mai, T.; Zhang, Q. M. Appl Phys Lett 2001, 78, 2360.
4. (a) Chu, B. J.; Zhou, X.; Neese, B.; Zhang, Q. M. IEEE Trans Dielectr Electr Insul 2006, 13, 1162; (b) Bauer, F.; Fousson, E.; Zhang, Q. M. IEEE Trans Dielectr Electr Insul 2006, 13, 1149; (c) Chu, B. J.; Zhou, X.; Ren, K. L.; Neese, B.; Lin, M. R.; Wang, Q.; Bauer, F.; Zhang, Q. M. Science 2006, 313, 334; (d) Zhang, Z. C.; Chung, T. C. M. Macromolecules 2007, 40, 783; (e) Zhang, Z. C.; Chung, T. C. M. Macromolecules 2007, 40, 9391; (f) Zhang, Z. C.; Meng, Q. J.; Chung, T. C. M. Polymer 2009, 50, 707.
5. (a) Ma, W. Z.; Zhang, J.; Chen, S. J.; Wang, X. L. Appl Surf Sci 2008, 254, 5635; (b) Mijovic, J.; Sy, J. W.; Kwei, T. K. Macromolecules 1997, 30, 3042; (c) Ma, W. Z.; Zhang, J.; Wang, X. L. Appl Surf Sci 2008, 254, 2947; (d) Liu, J. P.; Jungnickel, B. J. J Polym Sci Part B: Polym Phys 2006, 44, 338; (e) Elashmawi, I. S.; Hakeem, N. A. Polym Eng Sci 2008, 48, 895; (f) Kalivianakis, P.; Jungnickel, B. J. J Polym Sci Part B: Polym Phys 1998, 36, 2923; (g) Ma, W. Z.; Zhang, J.; Wang, X. L.; Wang, S. M. J Appl Surf Sci 2007, 253, 8377; (h) Yoshida, H. J Therm Anal 1997, 49, 101.
6. (a) Gregorio, R. J Appl Polym Sci 2006, 100, 3272; (b) Gregorio, R.; Cestari, M. J Polym Sci Part B: Polym Phys 1994, 32, 859; (c) Cortili, G.; Zerbi, G. Spectrochem Acta A 1967, 23, 285; (d) Kobayashi, M.; Tashiro, K.; Tadokoro, H. Macromolecules 1975, 8, 158; (e) Prest, W. M.; Luca, D. J. J Appl Phys 1975, 46, 4136; (f) Gregorio, R.; Capitao, R. C. J Mater Sci 2000, 35, 299.
7. Bormashenko, Y.; Pogreb, R.; Stanevsky, O.; Bormashenko, E. Polym Test 2004, 23, 791.
8. Salimi, A.; Yousefi, A. A. J Polym Sci Part B: Polym Phys 2004, 42, 3487.
9. (a) Song, D. D.; Yang, D. C.; Feng, Z. L. J Mater Sci 1990, 25, 57; (b) Gregorio, R.; Nociti, N. C. P. S. J Phys D: Appl Phys 1995, 28, 432; (c) Kim, K. J.; Cho, Y. J.; Kim, Y. H. Vib Spectrosc 1995, 9, 147.
10. Lovinger, A. J.; Davis, D. D.; Cais, R. E.; Kometani, J. M. Polymer 1987, 28, 617.
11. (a) Yang, D. C.; Thomas, E. L. J Mater Sci Lett 1984, 3, 929; (b) Yang, D. C.; Thomas, E. L. J Mater Sci Lett 1987, 6, 593.
12. Zhou, X. X.; Cakmak, M. J Macromol Sci Phys 2007, 46, 667.
13. Sy, J. W.; Mijovic, J. Macromolecules 2000, 33, 933.
14. Lu, F. J.; Hsu, S. L. Macromolecules 1986, 19, 326.